Journal of Membrane Science 543 (2017) 1–9

Contents lists available at ScienceDirect

Journal of Membrane Science

journal homepage: www.elsevier.com/locate/memsci

Study of the dual role mechanism of water-soluble additive in low temperature thermally-induced phase separation

Hao Zhang[b,c], Xiaolong Lu[a,b,c,*], Zhiyu Liu[b,c], Zhong Ma[b,c], Song Wu[b,c], Zhendong Li[b,c], Xiao Kong[b,c], Chunrui Wu[a,b,c,*]

[a] State Key Laboratory of Separation Membranes and Membrane Processes, Tianjin Polytechnic University, Tianjin 300387, PR China
[b] School of Material Science and Engineering, Tianjin Polytechnic University, Tianjin 300387, PR China
[c] Institute of Biological and Chemical Engineering, Tianjin Polytechnic University, Tianjin 300387, PR China

ARTICLE INFO

Keywords:
PVDF
L-TIPS
Water-soluble non-solvent
Liquid-liquid phase separation
Tensile strength

ABSTRACT

In the NIPS method, polyethylene glycol-400 (PEG400) was a common water-soluble additive and usually played the role of a pore-forming agent due to NIPS double-diffusion. In this paper, the new role of non-solvent PEG400 in the low temperature thermally-induced phase separation (L-TIPS) was analyzed. PEG400 were used to regulate the phase separation mechanism of the dope solution, and then to improve the membrane structure and performance. The membrane structure was regulated by gradually increasing the PEG400 content, the role evolution of water-soluble non-solvent PEG400 on the phase transformation mechanism and the effect on tensile strength of the polyvinylidene fluoride (PVDF) membrane were studied. The results show that the increase of PEG400 content can increase the cloud point temperature of dope solution, accelerate the thermally induced phase separation (TIPS) effect and inhibit the negative effect of the non-solvent induced phase separation (NIPS) effect on membrane structure. Meanwhile, the increase of PEG400 content can shift the TIPS effect of the dope solution system from solid-liquid phase separation to liquid-liquid phase separation and inhibit the growth of PVDF spherulites during the TIPS process. The dual role mechanism of PEG400 together eliminates the NIPS finger-like voids and the TIPS sphere-packed aggregation structure, which have the negative impact on tensile strength of the PVDF membrane. The PVDF membrane shows excellent mechanical properties; the tensile strength of the membrane reaches 3.12 MPa (more than 3–6 times higher than the membranes reported), pure water flux reaches 391 L m^{-2} h^{-1}, and the rejection rate of carbon ink is 100%.

1. Introduction

The preparation of high-performance polyvinylidene fluoride (PVDF) membranes is a focus of the water treatment field [1–5]. Traditional membrane preparation methods primarily include non-solvent induced phase separation (NIPS) [6–10] and thermally induced phase separation (TIPS) methods [11–15]. The NIPS method, although simple, usually forms a large number of finger-like voids in the membrane due to double-diffusion, resulting in insufficient membrane mechanical properties [6–10]. The TIPS method is able to prepare high-mechanical-strength membranes; however, the formation temperature is generally above the fusion point of the polymer. The homogeneous dope solution is formed by mixing the molten polymer (for PVDF, the melting point is 172 °C) with the high temperature diluent. Therefore, problems such as high energy consumption and stringent requirements of membrane preparation equipment [11–15] arise. In addition, the PVDF membrane prepared via TIPS method is easy to form sphere-packed aggregation structure due to solid-liquid phase separation, the tensile strength of the membrane is also not satisfactory. Owing to most water-soluble diluents having lower relative heat stabilities, they can hardly be used in TIPS. Therefore, the choice of diluent to regulate the membrane structure is usually water-insoluble. The post-treatment process needs to use a two-step method, i.e., extracting the diluent via a non-water coagulating bath (the coagulation bath is usually ethanol), then further post-treatment via water. The process is cumbersome, and is also not conducive to environmental protection [16–18].

To solve the problems in the NIPS and TIPS methods, Japanese scholars Akihiro and Hideki [19] found a method that can prepare the TIPS membrane with high mechanical strength at a lower formation temperature (the formation temperature is lower than the melting point of the polymer, melting polymer is unnecessary, it is enough to prepare homogeneous dope solution only through dissolving polymer with diluent). They put forward the concept of water-soluble latent solvent in their 2007 patent, i.e., the water-soluble solvent had a poor ability to

* Corresponding authors at: State Key Laboratory of Separation Membranes and Membrane Processes, Tianjin Polytechnic University, Tianjin 300387, PR China.
E-mail addresses: luxiaolong@263.net (X. Lu), wuchunrui@tjpu.edu.cn (C. Wu).

http://dx.doi.org/10.1016/j.memsci.2017.08.032
Received 10 May 2017; Received in revised form 20 July 2017; Accepted 12 August 2017
Available online 15 August 2017

dissolve the polymer at room temperature; however, with increasing temperature, it can form a homogeneous solution with a high concentration of polymer. They analyzed the water-soluble latent solvents of PVDF such as γ-butyrolactone, propylene carbonate, and triethyl phosphate. Based on the water-soluble latent solvent, they prepared PVDF membranes with excellent comprehensive performance at 140–160 °C. Although they did not provide the specific preparation method, the progress from water-insoluble diluent to water-soluble latent solvent was a breakthrough in the TIPS formation method. Lu [20] named this method the low temperature thermally-induced phase separation (L-TIPS) and gave a more specific definition: the polymer and the diluent in a homogeneous solution at a temperature below the fusion point of the polymer. During phase inversion membrane formation, the dope solution is kept at a temperature below this fusion point but above the cloud point of the dope solution. Additionally, the coagulating bath temperature is significantly below the cloud point of the dope solution. Thus, both TIPS and NIPS phase separation mechanisms will operate when the dope solution enters the water coagulating bath.

A few studies on PVDF membrane prepared via L-TIPS method have been reported [21,22]. However, when the coagulation bath is water, the membrane will still form sphere-packed aggregation structure due to solid-liquid phase separation, which has a negative impact on the tensile strength of the membrane. The attempt to eliminate the sphere-packed aggregation structure by altering the coagulating condition and the cooling rate entails complicated post-treatment and environmental pollution but also resulted in a mediocre tensile strength. Therefore, it is worth researching how to start from diluent, using water-soluble diluent to regulate the phase separation mode of the membrane formation system, which in turn helps eliminate the sphere-packed aggregation structure in the membrane and improve the tensile strength. yet, so far no report on this has been found in the literature. Through this simple and effective method, water can be directly used as the coagulation bath to extract diluent in the post-treatment process. Meanwhile, it can provide convenience and possibility for the hydrophilic modification of the membrane, which is useful in the application of the membrane.

In this paper, the PVDF flat membrane was prepared via L-TIPS method with water-soluble solvent triethyl phosphate (TEP) and conventional water-soluble non-solvent PEG400 as mixed diluent. Among them, TEP was suitable for the L-TIPS method due to the low compatibility with PVDF at low temperature and the good compatibility with L-TIPS at high temperature. PEG400 was used to regulate the membrane structure. The method of covering both sides of the dope solution with polyimide film was used to prevent dissolution of PEG400 out from the dope solution due to NIPS double diffusion during the membrane formation process. The occurrence mechanisms of TIPS and NIPS processes in L-TIPS membrane formation were regulated by changing the PEG400 content. The role evolution of PEG400 on the phase transformation mechanism and the effect on tensile strength of the PVDF membrane are studied. The effect of the role evolution on the structure and performance of the membranes is also discussed.

2. Materials and methods

2.1. Materials

Polyvinylidene fluoride (PVDF): industrial grade, Solvay Specialty Polymers, Solvay Solexis Company in France. Polyethylene glycol (PEG400): analytical pure grade, Tianjin Kermel Chemical Reagent Co., Ltd. Triethyl phosphate (TEP): analytical pure grade, Tianjin Guangfu Fine Chemical Research Institute. Polydimethylsiloxane: analytical pure grade, Tianjin Fengchuan Chemical Reagent Co., Ltd. Carbon ink: Tianjin Ostrich-Ink Company.

Table 1
The mass ratio of dope solution system containing PVDF/PEG400/TEP.

	Dope solution sample	PEG400(g)	TEP(g)
1	D25-0	–	75.0
2	D25-10%	7.5	67.5
3	D25-20%	15.0	60.0
4	D25-33%	25.0	50.0
5	D25-38%	28.5	46.5
6	D25-42%	31.5	43.5
7	D25-46%	34.5	40.5
8	D25-50%	37.5	37.5
9	D25-54%	40.5	34.5

Note: the PVDF content of the four dope solutions is 25.0 g.

2.2. Preparation of dope solution system containing PVDF/PEG400/TEP

Dope solutions of PVDF/PEG400/TEP system were prepared and the composition of each dope is listed in Table 1. In this study, the content of PVDF relative to the total dope solution was 25%. At 160 °C, the maximum content of water-soluble non-solvent PEG400 at which the dope solution can be formed in the mixed diluent is 54%. Before being allowed to stand for defoaming (oil bath was polydimethylsiloxane), the dope solutions (Table 1) were stirred for 3 h at 160 °C. At this time, the dope solutions had a transparent and uniform state which proved that PVDF had been fully dissolved. After that, the prepared solutions were introduced into test tubes (preheated at 160 °C). The test tubes containing the solutions were cooled in liquid nitrogen and sampled. The dope solution systems were named D25-0, D25-10%, and so on based on the content of PVDF in the total solution and the content of non-solvent additive PEG400 in the mixed diluent.

2.3. Preparation of PVDF membranes

D25-0, D25-10%, D25-33%, and D25-54% samples were placed at the center of two polyimide films and pressed into a mold preheated beforehand at 160 °C. The membrane formation pressure was 4 MPa and the thickness of the membrane was 0.30 mm. The products were then immediately put into 10 °C water coagulation bath. After 20 s, the polyimide film on the upper side of the sample was removed, and the sample was directly contacted with the coagulation bath to solidify into a membrane. The membranes were named M25-0, M25-10%, M25-33%, and M25-54%, respectively. The schematic diagram of membrane formation equipment is illustrated in Fig. 1.

2.4. Scanning electron microscopy

The membranes were freeze-fractured in liquid nitrogen, plated with gold, and observed under a S-4800 field emission scanning electron microscopy (FE-SEM) (Hitachi, Japan).

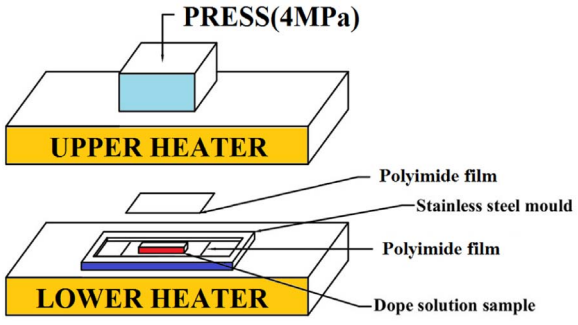

Fig. 1. The schematic diagram of membrane formation equipment.

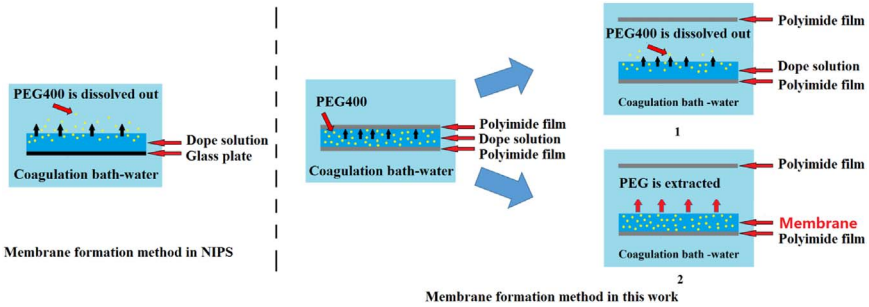

Fig. 2. The state of PEG400 in different membrane formation methods.

2.5. Cloud point

Cloud point measurements of all dope solution samples cooled by liquid nitrogen were carried out on a BX51 hot stage optical microscope (Olympus Corporation, Japan): the dope solution samples were placed between a pair of microscope cover slips and a Teflon film with a circle opening in the center was inserted between the cover slips to prevent diluent loss by evaporation, then heated up to 180 °C with a heating rate of 40 °C min^{-1} and kept the temperature for 3 min. After that, the dope solution samples were cooled to 10 °C with a cooling rate of 10 °C min^{-1}, optical microscope was used to observe the cloud point, the cloud point temperatures were recorded and the photomicrographs of dope solutions were photographed at 10 °C. During the cooling process, if the droplets appear and the cross extinction does not occur, the dope solution occurs liquid-liquid phase separation. If the cross extinction occurs, it will be considered as a phenomenon typical of spherulite formation. At this point, the dope solution occurs solid-liquid phase separation.

2.6. Pure water flux

Laboratory-made ultrafiltration membrane evaluation device was employed to determine the permeation flux of the membranes. The membranes were pre-pressed at 0.15 MPa for 20 min, then volume of permeation was filtrated at 0.1 MPa transmembrane pressures for 10 min at 20 °C and permeation was then calculated as following [23]:

$$J = \frac{V}{S \times t} = \frac{V}{\pi\left(\frac{d}{2}\right)^2 \times t} \quad (1)$$

where J is the permeation flux (L m^{-2} h^{-1})), V is the volume of water filtrated (L), S is the effective area of the separation membrane (m^2), d is the diameter of the effective area (m) and t is the test time (h). Each sample was tested 5 times to get an arithmetic mean.

2.7. Pore size distribution

Pore size distributions of the membranes were measured by a Porolux 1000 Capillary flow pore size analyzer (Porometer, Germany).

2.8. Mechanical properties

Mechanical Properties of the membranes were tested with a CMT4503 PC-controlled electronic universal testing machine (MTS industrial system Co., Ltd., China). The 30 mm-long, 20 mm-wide membranes were used for test. The tests were carried out at 25 °C at a tensile rate of 10 mm min^{-1}. Each sample was tested 5 times to get an arithmetic mean.

2.9. Rejection

The performances of the membranes in rejecting carbon ink were measured by the laboratory-made ultrafiltration membrane evaluation device. The feed solution was 1 g L^{-1} carbon ink solution, the transmembrane pressure was 0.040 MPa (the inlet and outlet pressure were 0.10 MPa and 0.060 MPa, respectively). The distribution of ink particles in the feed and permeate solutions was analyzed by Zetasizer Nano ZS90 particle size distribution analyzer (Malvern, Britain)

3. Results and discussion

3.1. Effect of water-soluble non-solvent PEG400 on morphology of PVDF membrane

To eliminate the sphere-packed aggregation structure, which has a negative impact on tensile strength of the membrane, water-soluble additive PEG400 was used to regulate the membrane structure. When the coagulation bath is water, in the NIPS method PEG400 usually plays the role of a pore-forming agent during the membrane formation process due to double-diffusion (Fig. 2: membrane formation method in NIPS). In the L-TIPS method, both TIPS and NIPS phase separation mechanisms occur during the formation process [24]. Therefore, PEG400 (the pore-forming agent) is also dissolved out due to NIPS double-diffusion. Thus, PEG400 cannot play the role of eliminating the sphere-packed aggregation structure of the membrane. To prevent the occurrence of this condition, we prepared the PVDF flat membrane by covering both sides of the dope solution with polyimide film. When the dope solution is immersed in a water coagulation bath, this method can prevent the rapid dissolution out of PEG400 during the initial stage process of membrane formation, and make it play the role in the elimination (Fig. 2: membrane formation method in this work). At this time, the dope solution system will only occur the TIPS effect. When the dope solution is immersed in water for a certain period of time (20 s), we removed the upper side polyimide film of dope solution, at this time, if the TIPS effect has not finished, the dope solution has not solidified into a membrane, the dope solution will occur the NIPS effect due to water coagulation bath and solidify into a membrane (Fig. 2: membrane formation method 1 in this work). If the TIPS effect has finished, the dope solution has solidified into a membrane, the dope solution will not occur the NIPS effect, the water coagulation bath only plays a role of diluent extraction (Fig. 2: membrane formation method 2 in this work).

Fig. 3 shows the SEM morphologies of the PVDF membranes (M25-0, M25-10%, M25-33%, and M25-54%). The arrows in Fig. 3 indicate the upper surface of the PVDF membranes. It can be seen that when the dope solution has no PEG400, on the upper surface of M25-0, there is a skin structure with less voids. Near the upper surface of the cross-section of M25-0, there is a thick dense structure, which is free of finger-like voids. When the dope solution has a small amount of PEG400, some voids appear on the upper surface of M25-10%. Near the upper surface of the cross-section of M25-10%, the dense structure becomes thinner and contains micro finger-like voids. With the increase of PEG400 content in the mixed diluent, on the upper surface of M25-33%, the skin structure disappears and macrovoids appear. The cross-section of M25-33% forms a non-dense sphere-packed aggregation structure and the finger-like voids disappear. With further increase in the content of PEG400 in the mixed diluent, on the upper surface of M25-54%, the

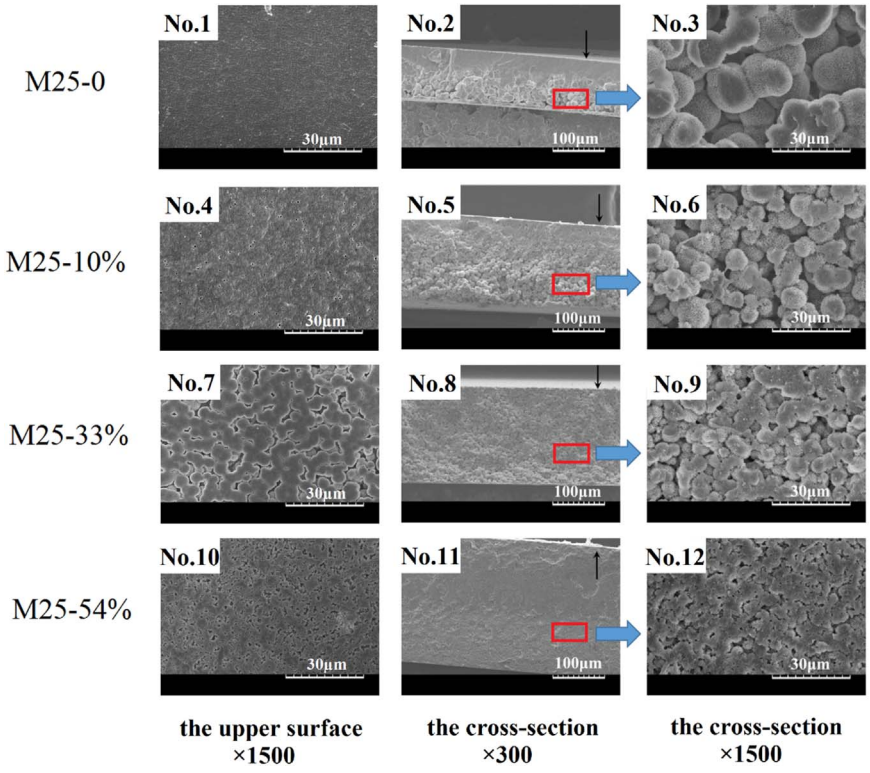

Fig. 3. The SEM morphologies of the membranes.

Table 2
Temperature difference between coagulation bath temperature and cloud point temperature of dope solution with different PEG400 content.

	The content of PEG400 in the mixed diluent	Cloud point temperature (°C)	Temperature difference (°C)
D25-0	non-existent	15	5
D25-10%	10%	37	27
D25-33%	33%	90	80
D25-54%	54%	151	141

Note: the coagulation bath temperature of the four dope solutions is 10 °C.

macrovoids decrease. There is neither a dense structure nor finger-like voids on the cross-section of M25-54%. Table 2 shows temperature difference between coagulation bath temperature and cloud point temperature of dope solution with different PEG400 content. By analyzing Fig. 2 and Table 2, for D25-0, when the dope solution is immersed in the water coagulation bath, the temperature difference between coagulation bath and cloud point of D25-0 is very small (5 °C). At this time, the TIPS effect occurs very slowly. After D25-0 is immersed in water for 20 s, the system has not yet solidified into a membrane due to the TIPS effect. Therefore, when the polyimide film on the upper side of dope solution was removed, the NIPS effcet begins to occur (Fig. 2: membrane formation method 1 in this work). Owing to D25-0 without

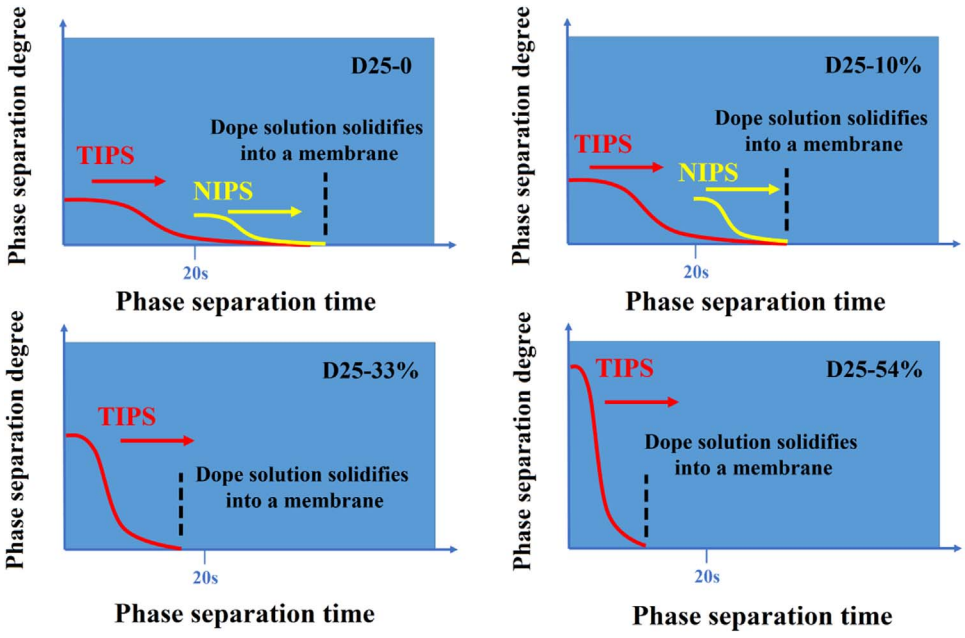

Fig. 4. The occurrence mechanism of the TIPS process and the NIPS process in the L-TIPS method.

Table 3
Hansen solubility parameters of PVDF, PEG400 and TEP.

	δ_d ($MPa^{1/2}$)	δ_p ($MPa^{1/2}$)	δ_h ($MPa^{1/2}$)	δ_t ($MPa^{1/2}$)
PVDF	17.20[a]	12.50[a]	9.20[a]	23.20[a]
PEG400	16.60[b]	3.70[b]	13.30[b]	21.60[b]
TEP	16.80[a]	11.50[a]	9.20[a]	22.30[a]

[a] Ref. [26].
[b] Ref. [27].

PEG400, M25-0 forms a skin structure with less voids on the upper surface [25]. Similar to the case of D25-0, when D25-10% is immersed in the water coagulation bath, the temperature difference between coagulation bath and cloud point of D25-10% is also very small (27 °C). At this time, the TIPS effect occurs also very slowly. After D25-10% is immersed in water for 20 s, the system has also not yet solidified into a membrane due to the TIPS effect. When the polyimide film on the upper side of dope solution was removed, the NIPS effcet occurs, which leads to the dope solution solidifying into a membrane. At this point, the small amount of PEG400 in the dope solution plays a role as a pore-forming agent and PEG400 is dissolved out when double-diffusion occurs, which leads to a thinner dense structure near the upper surface and the appearance of micro finger-like voids. For M25-33%, with the increase of PEG400 content in the mixed diluent, the temperature difference between coagulation bath and cloud point of D25-33% obviously increases (80 °C). At this time, when D25-33% is immersed in the water coagulation bath, the TIPS effect is significantly accelerated. After D25-33% is immersed in water for 20 s, the dope solution has been solidified due to the TIPS effect. When the polyimide film on the upper side of dope solution was removed, the NIPS effect will not occur. At this point, solvent triethyl phosphate and water-soluble non-solvent PEG400 are extracted only as a diluent for TIPS (Fig. 2: membrane formation method 2 in this work). Therefore, no finger-like voids—caused by double-diffusion during the NIPS method—develop near the upper surface. Similarly, for M25-54%, with further increase in the content of PEG400 in the mixed diluent, the temperature difference between coagulation bath and cloud point of D25-54% increases further (141 °C). When D25-54% is immersed in the coagulation bath, the TIPS effect is accelerated further. Therefore, no finger-like voids, which are caused by PEG400 dissolving out in the NIPS method, develop near the upper surface. Fig. 4 shows the occurrence mechanisms of TIPS and NIPS processes of the four membranes during the immersion process. Among them, D25-0 and D25-10% will occur the TIPS effect and the NIPS effect successively, D25-33% and D25-54% will only occur the TIPS effect. In summary, the increase of PEG400 content can effectively promote the transformation of phase separation process from NIPS to TIPS.

It can also be seen from Fig. 3 that the figure (showing cross-section morphologies at the same magnification factor (×300)) demonstrates the growing thickness of the membranes M25-0 (0.18 mm), M25-10% (0.20 mm), M25-33% (0.28 mm) and M25-54% (0.28 mm) (the wet membrane thickness of the four membranes is measured by vernier caliper). Among them, there is a big difference between the wet membrane thickness of the first two membranes and the initial membrane formation thickness (0.30 mm). However, the wet membrane thickness of the last two membranes and the initial membrane formation thickness are almost the same. By analyzing the membrane formation process, the NIPS effects of M25-0 and M25-10% during the membrane formation cause the dissolution out of the solvent and non-solvent in the dope solution. Therefore, compared with the initial membrane thickness, the wet membrane thickness of M25-0 and M25-10% becomes thinner obviously. M25-33% and M25-54% only occur the TIPS effect during the membrane formation. Because there is no exchange process between solvent and non-solvent before membrane formation, compared with the initial membrane thickness, there is little change in the wet membrane thickness of M25-0 and M25-10%.

It can also be seen from Fig. 3 that as the content of PEG400 in the mixed diluent grows, the sphere-packed aggregation structure diminishes gradually on the cross-section of M25-0, M25-10%, M25-33%, and M25-54% until it completely disappeared. This result shows that the increase of PEG400 content can not only promote the transformation of phase separation process from NIPS to TIPS, but also shift the TIPS effect of the dope solution system from solid-liquid phase separation to liquid-liquid phase separation, and then eliminate the sphere-packed aggregation structure which is easy formed during TIPS process.

3.2. Effect of water-soluble non-solvent PEG400 on phase separation of the dope solution

In summary, the increase of PEG400 content increases the cloud point temperature of dope solution. The increase of the temperature difference between cloud point and coagulation bath accelerates the TIPS effect, this result is consistent with common sense. At the same time, the increase of PEG400 content also eliminates the sphere-packed aggregation structure which is easy formed during TIPS process. To investigate the mechanism of eliminating the sphere-packed aggregation structure on the membrane cross-section caused by PEG400, we investigated the effect of the increase of PEG400 content on phase separation of the dope solution. Combining the solubility parameters of PVDF, PEG400, and TEP in Table 3, Table 4 shows the calculated value of the solubility parameter of the mixed diluent in a variety of dope systems (δ_{dm}, δ_{pm}, δ_{hm}, δ_{tm}) and the change in Gibbs free energy (ΔG^E).

The calculated value of the solubility parameter of the mixed diluent (δ_{dm}, δ_{pm}, δ_{hm}, δ_{tm}) was obtained from the following formula [28] :

$$\begin{cases} \delta_{dm} = \delta_{dPEG400}\varphi_{PEG400} + \delta_{dTEP}\varphi_{TEP} \\ \delta_{pm} = \delta_{pPEG400}\varphi_{PEG400} + \delta_{dTEP}\varphi_{TEP} \\ \delta_{hm} = \delta_{hPEG400}\varphi_{PEG400} + \delta_{hTEP}\varphi_{TEP} \\ \delta_{tm} = \delta_{tPEG400}\varphi_{PEG400} + \delta_{tTEP}\varphi_{TEP} \end{cases} \quad (3)$$

where m stands for mixed diluent, d, p, and h stand for the dispersion force, polar force, and hydrogen bond components, respectively, $\delta_t = \sqrt{\delta_d^2 + \delta_p^2 + \delta_h^2}$, and φ stands for the content of the single diluent accounting for mixed diluent.

The change value of Gibbs free energy ΔG^E was obtained by the following formula:

$$\Delta G^E = (\delta_{dm} - \delta_{dPVDF})^2 + (\delta_{pm} - \delta_{pPVDF})^2 + (\delta_{hm} - \delta_{hPVDF})^2 \quad (4)$$

ΔG^E is used to characterize the compatibility of the mixed diluent with PVDF. A smaller value of ΔG^E indicates better compatibility of the mixed diluent with PVDF [29]. At the same content of PVDF, increasing the content of PEG400 in the mixed diluent increased ΔG^E from 1.16 J m^{-3} to 32.29 J m^{-3} (Table 4), indicating that the compatibility between the mixed diluent and PVDF became worse. When the

Table 4
The calculated values of Hansen solubility parameters of different mixed diluents and ΔG^E.

	Dope solution sample	δ_{dm} ($MPa^{1/2}$)	δ_{pm} ($MPa^{1/2}$)	δ_{hm} ($MPa^{1/2}$)	δ_{tm} ($MPa^{1/2}$)	ΔG^E (J/m^3)
1	D25-0	16.80	11.50	9.20	22.30	1.16
2	D25-10%	16.78	10.72	9.61	22.23	3.51
3	D25-20%	16.76	9.94	10.02	22.16	7.42
4	D25-33%	16.73	8.90	10.56	22.07	15.03
5	D25-38%	16.72	8.54	10.76	22.03	18.35
6	D25-42%	16.72	8.22	10.92	22.01	21.51
7	D25-46%	16.71	7.91	11.09	21.98	24.88
8	D25-50%	16.70	7.60	11.25	21.95	28.46
9	D25-54%	16.69	7.29	11.41	21.92	32.29

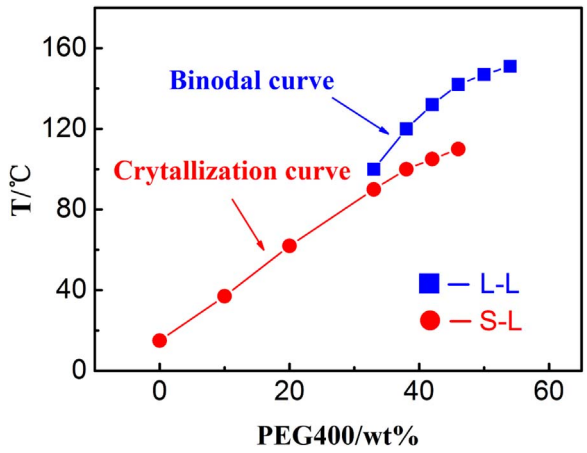

Fig. 5. The phase diagram of the dope solution system. L-L: L-L phase separation; S-L: S-L phase separation.

compatibility of the dope solution system is worse, liquid-liquid phase separation is more likely to occur, i.e., compared with D25-0, D25-54% is more likely to undergo liquid-liquid phase separation. Fig. 5 shows a phase diagram of the dope solution system. It is clear from Fig. 5 that when the mixed diluent has no PEG400, D25-0 only occurs the solid-liquid phase separation. At this time, M25-0 will form a non-dense sphere-packed aggregation structure. With the increase of PEG400 content in the mixed diluent, the solid-liquid phase separation temperature (crystallizing point) increases gradually. When the PEG400 content is 33% in the mixed diluent, D25-33% begins to appear liquid-liquid phase separation, however, it will still enter solid-liquid phase separation very soon. At this time, due to the area between the binodal curve and the crystal curve is very small, M25-33% will still form a non-dense sphere-packed aggregation structure. With further increase in the content of PEG400 in the mixed diluent, the area between the binodal curve and the crystal curve increases further. When the PEG400 content is 54% in the mixed diluent, D25-54% only occurs the liquid-liquid phase separation and the solid-liquid phase separation does not occur, in agreement with the prediction in Table 4. At this time, M25-54% eliminates the sphere-packed aggregation structure. In summary, the increase of PEG400 content promotes the transformation of phase separation process, shifts the dope solution from solid-liquid phase separation to liquid-liquid phase separation and eliminates the sphere-packed aggregation structure, which has a negative impact on tensile strength of the PVDF membrane.

3.3. Effect of water-soluble non-solvent PEG400 on crystal structures of PVDF

In view of the phenomenon that the solid-liquid phase separation completely disappeared during the phase separation process of D25-54% (Fig. 5), this study investigated the effect of the water-soluble non-solvent PEG400 on PVDF spherulite. Fig. 6 shows microphotographs of the D25-0 and D25-54% systems. Fig. 6 suggests apparent cross extinction in the cooling process of D25-0, a phenomenon typical of spherulite formation due to solid-liquid phase separation. With D25-54%, however, as the temperature drops, the dope solution only occurs liquid-liquid phase separation, the phenomenon of droplet growth is observed only in the microphotograph.

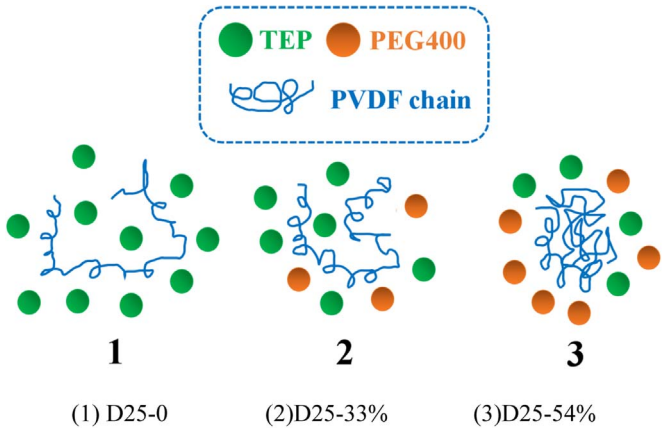

Fig. 7. Schematic diagram of the state of the PVDF chain in PEG400/TEP mixed diluent.

By analyzing Fig. 6, it is seen that the PVDF spherulite was inhibited by the water-soluble non-solvent PEG400. In the crystalline polymer solution, the growth size of spherulite depends on the time for crystallization and the space available for nucleation growth [30,31]. Fig. 7 shows a schematic diagram of the state of the PVDF chain in the PEG400/TEP mixed diluent. When the water-soluble non-solvent PEG400 content is low, PVDF chain segments may extend comfortably in good solvent, which enables the system to have fewer nucleating points, i.e., more space for growth. Meanwhile, when D25-0 is immersed in the water coagulation bath, due to the TIPS effect occurs very slowly, the system needs a longer time to solidify into a membrane. In such a case, D25-0 may develop a perfect spherulite structure (Fig. 7:1). At a higher content of PEG400, PVDF chain segments have more nucleating points in the non-solvent, reducing the space for crystal growth. Meanwhile, due to the increase of PEG400 content accelerates the TIPS effect, the system needs less time to solidify into a membrane, also hindering the growth of spherulite. In this case the system may develop a imperfect microcrystalline structure (2:D25-10%). When the content of PEG400 reaches a certain level, under the influence of non-solvent the entanglement of PVDF chain segments occurs very quickly; additionally, an excessive number of nucleating points develop on the PVDF chain segments leaving insufficient time and space for spherulite growth, and in this case no spherulite structures are developed (3:D25-54%).

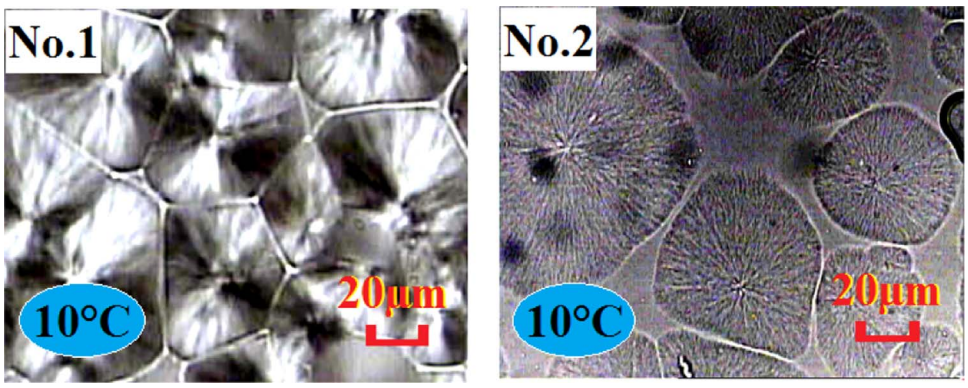

Fig. 6. Microphotographs of the dope solution (No.1: D25-0, No.2: D25-54%).

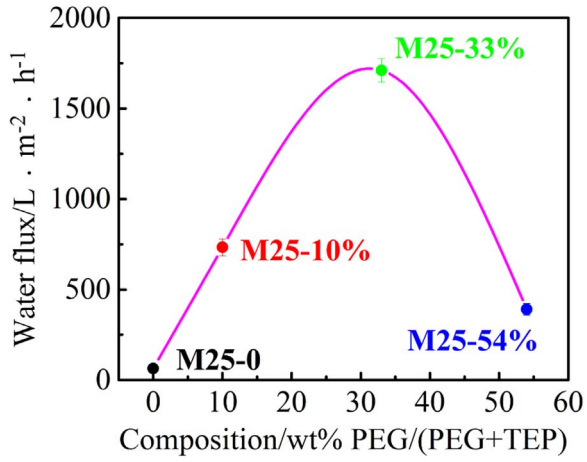

Fig. 8. The pure water flux of the membranes.

In summary, the increase of water-soluble non-solvent PEG400 content can inhibit the growth of PVDF spherulites during the TIPS process. When the PEG400 content in the mixed diluent reaches 54%, the sphere-packed aggregation structure of the membrane is disappeared.

3.4. Effect of water-soluble non-solvent PEG400 on performance of PVDF membrane

3.4.1. Effect of water-soluble non-solvent PEG400 on pure water flux of PVDF membrane

Fig. 8 shows the pure water flux of M25-0, M25-10%, M25-33%, and M25-54%. The flux of the four membranes follows the order M25-33% > M25-10% > M25-54% > M25-0 at a certain transmembrane pressure. In view of the cross-section morphologies of the membranes (Fig. 6) and pore sizes (Fig. 9), it is known that due to dope solution without PEG400, M25-0 has a thick and dense structure, leading to a low membrane pure water flux of 64 L m^{-2} h^{-1}. Owing to the small amount of PEG400 in the dope solution plays a role as a pore-forming agent, M25-10% eliminates the thick dense structure near the upper surface and appears micro finger-like voids. Additionally, due to the large number of sphere-packed aggregation structure of M25-10% reduces the permeable resistance of the membrane, the pure water flux of M25-10% increases to 733 L m^{-2} h^{-1}. With the increase of PEG400 content in the mixed diluent, during the membrane formation process, the TIPS effect of M25-33% is significantly accelerated, the dope solution only occurs the solid-liquid phase separation caused by the TIPS effect. The membrane is free of dense structure and the cross-section is of a sphere-packed aggregation structure. Therefore, the most probable pore size is 585 nm and the pore size distribution is wide, suggesting the pore structure of M25-33% is mainly formed by cavities in the sphere-packed aggregation structure; this leads the membrane pure water flux to increase further to 1711 L m^{-2} h^{-1}. With further increase in the content of PEG400 in the mixed diluent, PEG400 shift the dope solution from solid-liquid phase separation to liquid-liquid phase separation and inhibit the growth of PVDF spherulites during the TIPS process. M25-54% eliminates the sphere-packed aggregation structure in the membrane, the membrane has a narrow pore size distribution and the most probable pore size is 168 nm, explaining the apparent drop in pure water flux (391 L m^{-2} h^{-1} at 0.1 MPa) relative to that of M25-33%. In summary, the regulation of membrane structure caused by the dual role mechanism of PEG400 affects the pure water flux performance, with the increase of PEG400 content in the mixed diluent, the membrane eliminates the dense structure and the pure water flux increases obviously. However, to obtain the PVDF membrane with excellent comprehensive properties, we should also examine the mechanical properties of the membrane.

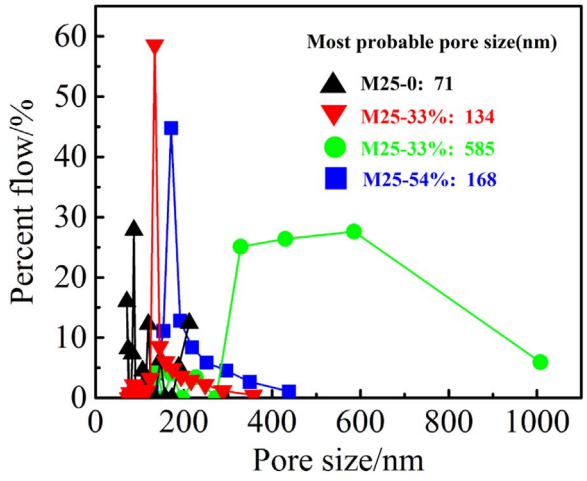

Fig. 9. The pore size distribution of the membranes.

3.4.2. Effect of PEG400 on mechanical properties of PVDF membrane

Table 5 shows the mechanical properties of M25-0, M25-10%, M25-33%, and M25-54%. It is clear from Table 5 that mechanical properties of the four membranes follows the order M25-54% > M25-0 > M25-10% > M25-33%. In view of the cross-section morphologies of the membranes (Fig. 6) and Table 5, it is known that M25-0 displays excellent mechanical properties, its tensile strength reaches 2.39 MPa, it is mostly attributable to the dope solution of M25-0 without pore-forming agent. With the increase of PEG400 content in the mixed diluent, the pore-forming role of PEG400 in the NIPS process make the membrane form a thinner dense structure and appear micro finger-like voids, which leads to obvious decrease of tensile strength of M25-10%, the tensile strength is 0.70 MPa. This phenomenon is consistent with the regular rule of NIPS pore-forming. With further increase in the content of PEG400 in the mixed diluent, during the membrane formation process, the TIPS effect of M25-33% is significantly accelerated, the dope solution only occurs the solid-liquid phase separation caused by the TIPS effect. At this time, the cross-section of M25-33% forms the sphere-packed aggregation structure, which leads to further decrease of tensile strength of M25-10%, the tensile strength is 0.51 MPa. When the PEG400 content in the mixed diluent is 54%, due to PEG400 eliminating the sphere-packed aggregation structure, M25-54% has the best mechanical indices among all the membranes, its tensile strength reaches 3.12 MPa. In summary, the regulation of membrane structure caused by the dual role mechanism of PEG400 also affects the mechanical properties. By analyzing Fig. 8 and Table 5, compared with M25-54%, the mechanical properties of M25-33% are obviously insufficient, even though it has the maximum pure water flux among all

Table 5
Comparison of mechanical properties of the membranes in this study (M25-0, M25-10%, M25-33% and M25-54%) and from literature (PVDF(25%), M25 and M-d30).

	Membrane thickness (mm)	Elastic modulus (MPa)	Elongation at break (%)	Tensile strength (MPa)
M25-0	0.18 ± 0.01	125.43 ± 7.39	41.41 ± 1.15	2.39 ± 0.03
M25-10%	0.20 ± 0.01	10.37 ± 1.13	33.41 ± 3.98	0.70 ± 0.08
M25-33%	0.28 ± 0.01	7.62 ± 0.87	19.78 ± 0.42	0.51 ± 0.17
M25-54%	0.28 ± 0.01	128.58 ± 8.24	56.63 ± 3.70	3.12 ± 0.09
PVDF(25%)[a]	–	–	–	1.60
M25[b]	–	59.39	14.87	1.47
M-d30[c]				1.21

[a] Ref. [3].
[b] Ref. [14].
[c] Ref. [32].

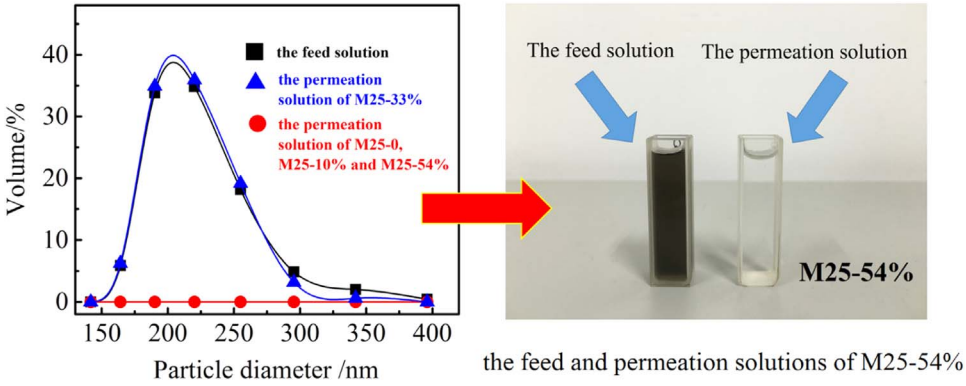

Fig. 10. The rejection effect of the membranes.

the membranes. Therefore, considering the comprehensive performance of membrane, M25-54% is a more excellent PVDF membrane.

It can also be seen from Table 5 that among the membranes reported in the literature that eliminate the sphere-packed aggregation structure by changing the coagulation bath environment, the tensile strength of M25-54% has an obvious advantage.

3.5. Effect of PEG400 on rejection of membrane

Finally, the performance of the membrane in rejecting carbon ink was tested. The particle size distributions of carbon in the feed and permeation solutions are shown in Fig. 10. The result shows that M25-0, M25-10% and M25-54% showed a good rejection performance due to the regulation of PEG400 on the structure. Carbon ink particles were completely rejected. However, M25-33% could hardly reject carbon ink particles in the feed solution. In view of the pore sizes (Fig. 9), we suspected that since the minimum particle size in the feed carbon ink solution was 0.164 μm (Fig. 10) and the most probable pore sizes of M25-0, M25-10% and M25-54% were 71 nm, 134 nm and 168 nm respectively, the membrane pores were blocked in the rejection process due to the bridging effect of carbon adsorption. This led to a complete rejection of the carbon particles and obvious decrease in flux. The most probable pore size of M25-33% was 585 nm, which was obviously larger than the maximum particle size (396 nm) of carbon ink in the feed solution. Therefore, M25-33% showed a poor rejection performance.

4. Conclusions

The new role of non-solvent PEG400 in the low temperature thermally-induced phase separation (L-TIPS) was analyzed. With the increase of PEG400 content, the TIPS effect can be accelerated and the negative effect of the NIPS effect on membrane structure can be inhibited. Meanwhile, the increase of PEG400 content can shift the TIPS effect of the dope solution system from solid-liquid phase separation to liquid-liquid phase separation and inhibit the growth of PVDF spherulites during the TIPS process. The dual role mechanism of PEG400 together eliminates the NIPS finger-like voids and the TIPS sphere-packed aggregation structure, which have the negative impact on tensile strength of the PVDF membrane.

When the PEG400 content in the mixed diluent was 54%, the PVDF membrane had the best mechanical indices among all the membranes and the tensile strength of the membrane reached 3.12 MPa (more than 3–6 times higher than the membranes reported), the pure water flux reached 391 L m^{-2} h^{-1}, and the rejection rate of carbon ink was 100%. The comprehensive performance of the membrane is excellent.

Acknowledgement

This study was supported by National Natural Science Foundation of China (21576210). Research Program of Application Foundation and Advanced Technology, Tianjin, China (15JCZDJC37500), Program for Changjiang Scholars and Innovative Research Team in University (PCSIRI) of Ministry of Education of China (Grand no. IRI13084), Marine Science and Technology Project of Tianjin Province (KJXH2014-03).

References

[1] W.Z. Lang, Q. Ji, J.P. Shen, et al., The roles of alkali metal counter-ions of PFSA play in the formation of PVDF/PFSA-M hollow fiber membranes, Desalination 292 (2012) 45–52.
[2] Z.Y. Song, M.H. Xing, J. Zhang, et al., Determination of phase diagram of a ternary PVDF/γ-BL/DOP system in TIPS process and its application in preparing hollow fiber membranes for membrane distillation, Sep. Purif. Technol. 90 (2012) 221–230.
[3] S. Rajabzadeh, C. Liang, Y. Ohmukai, et al., Effect of additives on the morphology and properties of poly(vinylidene fluoride) blend hollow fiber membrane prepared by the thermally induced phase separation method, J. Membr. Sci. 423–424 (2012) 189–194.
[4] M. Rahbari-Sisakht, A.F. Ismail, D. Rana, et al., Effect of SMM concentration on morphology and properties of surface modified PVDF hollow fiber membrane contactor for CO_2 absorption, Sep. Purif. Technol. 116 (2013) 67–72.
[5] F. Zhang, W.B. Zhang, Y. Yu, et al., Sol–gel preparation of PAA-g-PVDF/TiO2 nanocomposite hollow fiber membranes with extremely high water flux and improved antifouling property, J. Membr. Sci. 432 (2013) 25–32.
[6] A.M.R. Moghareh, S.C. Kumbharkar, A.M. Groth, et al., Ultrafiltration PVDF hollow fibre membranes with interconnected bicontinuous structures produced via a single-step phase inversion method, J. Membr. Sci. 407–408 (2012) 145–154.
[7] A.M.R. Moghareh, S.C. Kumbharkar, A.M. Groth, et al., Economical production of PVDF-g-POEM for use as a blend in preparation of PVDF based hydrophilic hollow fibre membranes, Sep. Purif. Technol. 106 (2013) 47–55.
[8] S. Simone, A. Figoli, A. Criscuoli, et al., Effect of selected spinning parameters on PVDF hollow fiber morphology for potential application in desalination by VMD, Desalination 344 (2014) 28–35.
[9] H. Zhang, X.Y. Hu, Y.B. Chen, et al., Highly permeable membrane prepared by phase inversion of mechanochemically modified polyvinylchloride, J. Mater. Sci. 49 (2014) 7290–7297.
[10] H. Zhang, X.Y. Hu, Y.B. Chen, et al., Dynamic rheological property and membrane formation of mechanochemically modified polyvinylchloride, J. Mater. Sci. 50 (2015) 4371–4378.
[11] Z.K. Li, W.Z. Lang, W. Miao, et al., Preparation and properties of PVDF/SiO2@GO nanohybrid membranes via thermally induced phase separation method, J. Membr. Sci. 511 (2016) 151–161.
[12] H.Q. Liang, Q.Y. Wu, L.S. Wan, et al., Polar polymer membranes via thermally induced phase separation using a universal crystallizable diluent, J. Membr. Sci. 446 (2013) 482–491.
[13] Z.L. Cui, N.T. Hassankiadeh, S.Y. Lee, et al., Tailoring novel fibrillar morphologies in poly(vinylidene fluoride) membranes using a low toxic triethylene glycol diacetate (TEGDA) diluent, J. Membr. Sci. 473 (2015) 128–136.
[14] Z.L. Cui, N.T. Hassankiadeh, S.Y. Lee, et al., Poly(vinylidene fluoride) membrane preparation with an environmental diluent via thermally induced phase separation, J. Membr. Sci. 444 (2013) 223–236.
[15] Z.L. Cui, E. Drioli, Y.M. Lee, Recent progress in fluoropolymers for membranes, Progress. Polym. Sci. 39 (1) (2014) 164–198.
[16] T. Ma, Z.Y. Cui, Y. Wu, et al., Preparation of PVDF based blend microporous membranes for lithium ion batteries by thermally induced phase separation: I. Effect of PMMA on the membrane formation process and the properties, J. Membr. Sci. 444 (2013) 213–222.
[17] Z.Y. Cui, Y.Y. Xu, L.P. Zhu, et al., Preparation of PVDF/PEO-PPO-PEO blend microporous membranes for lithium ion batteries via thermally induced phase separation process, J. Membr. Sci. 325 (2) (2008) 957–963.
[18] G.L. Ji, L.P. Zhu, B.K. Zhu, et al., Structure formation and characterization of PVDF

hollow fiber membrane prepared via TIPS with diluent mixture, J. Membr. Sci. 319 (2008) 264–270.
[19] A. Akihiro, Y. Hideki. Polyvinylidene Fluoride Hollow Yarn Type Microporous Film and Process for Production of the Same, WO/2007/080862.
[20] Z.P. Lu, X.L. Lu, C.R. Wu, et al., Preparation of polyvinylidene fluoride hollow fiber porous membrane via a low thermally induced phase separation, Membr. Sci. Technol. 32 (1) (2012) 12–22.
[21] B.J. Cha, J.M. Yang, Preparation of poly(vinylidene fluoride) hollow fiber membranes for microfiltration using modified TIPS process, J. Membr. Sci. 291 (1–2) (2007) 191–198.
[22] L. Wang, D.X. Huang, X.D. Wang, et al., Preparation of PVDF membranes via the low-temperature TIPS method with diluent mixtures: the role of coagulation conditions and cooling rate, Desalination 361 (2015) 25–37.
[23] J. Xu, Z.L. Xu, Poly(vinyl chloride) (PVC) hollow fiber ultrafiltration membranes prepared from PVC/additives/solvent, J. Membr. Sci. 208 (2002) 203–212.
[24] H. Matsuyama, Y. Takida, T. Maki, et al., Preparation of porous membrane by combined use of thermally induced phase separation and immersion precipitation, Polymer 43 (2002) 5243–5248.
[25] Z.C. Zhang, C.G. Guo, X.M. Li, et al., Effects of PVDF crystallization on polymer gelation behavior and membrane structure from PVDF/TEP system via modified TIPS process, Polym.-Plast. Technol. Eng. 52 (6) (2013) 564–570.
[26] A.F.M. Barton, CRC Handbook of Solubility Parameters and Other Cohesion Parameters, 2nd ed., CRC Press, Boca Raton, FL, 1991.
[27] B. Liu, Q.G. Du, Y.L. Yang, The phase diagrams of mixtures of EVAL and PEG in relation to membrane formation, J. Membr. Sci. 180 (2000) 81–92.
[28] A.F.M. Barton, Handbook of Solubility Parameters, CRC Press, Boca Raton, FL, 1983.
[29] G.L. Ji, C.H. Du, B.K. Zhu, et al., Preparation of porous PVDF membrane via thermally induced phase separation with diluent mixture of DBP and DEHP, J. Appl. Polym. Sci. 105 (2007) 1496–1502.
[30] X.J. Zhao, J. Cheng, S.J. Chen, et al., Controlled crystallization of poly(vinylidene fluoride) chains from mixed solvents composed of its good solvent and nonsolvent, J. Polym. Sci. Part B: Polym. Phys. 48 (2010) 575–581.
[31] D.I. Bower, An Introduction to Polymer Physics, Cambridge University Press, New York, 2002.
[32] G.L. Ji, B.K. Zhu, Z.Y. Cui, et al., PVDF porous matrix with controlled microstructure prepared by TIPS process as polymer electrolyte for lithium ion battery, Polymer 48 (2007) 6415–6425.